

## PDF hosted at the Radboud Repository of the Radboud University Nijmegen

The following full text is a publisher's version.

For additional information about this publication click this link.

<http://hdl.handle.net/2066/94094>

Please be advised that this information was generated on 2017-12-06 and may be subject to change.

## Single Molecule Fluorescence under Conditions of Fast Flow

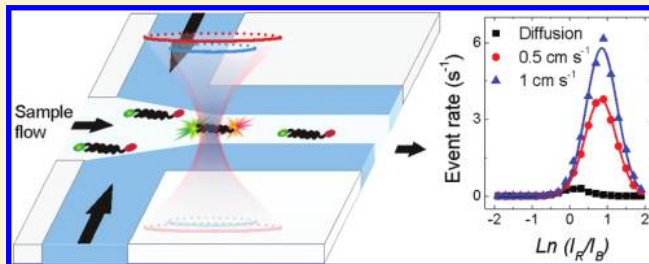
Mathew H. Horrocks, Haitao Li, Jung-uk Shim, Rohan T. Ranasinghe, Richard W. Clarke, Wilhelm T. S. Huck, Chris Abell, and David Klenerman\*

Department of Chemistry, University of Cambridge, Lensfield Road, Cambridge CB2 1EW, U.K.

Supporting Information

**ABSTRACT:** We have experimentally determined the optimal flow velocities to characterize or count single molecules by using a simple microfluidic device to perform two-color coincidence detection (TCCD) and single pair Förster resonance energy transfer (spFRET) using confocal fluorescence spectroscopy on molecules traveling at speeds of up to  $10 \text{ cm s}^{-1}$ . We show that flowing single fluorophores at  $\geq 0.5 \text{ cm s}^{-1}$  reduces the photo-physical processes competing with fluorescence, enabling the use of high excitation irradiances to partially compensate for the short residence time within the confocal volume ( $10\text{--}200 \mu\text{s}$ ).

Under these conditions, the data acquisition rate can be increased by a maximum of 38-fold using TCCD at  $5 \text{ cm s}^{-1}$  or 18-fold using spFRET at  $2 \text{ cm s}^{-1}$ , when compared with diffusion. While structural characterization requires more photons to be collected per event and so necessitates the use of slower speeds ( $2 \text{ cm s}^{-1}$  for TCCD and  $1 \text{ cm s}^{-1}$  for spFRET), a considerable enhancement in the event rate could still be obtained (33-fold for TCCD and 16-fold for spFRET). Using flow under optimized conditions, analytes could be rapidly quantified over a dynamic range of up to 4 orders of magnitude by direct molecule counting; a  $50 \text{ fM}$  dual-labeled model sample can be detected with 99.5% statistical confidence in around 8 s using TCCD and a flow velocity of  $5 \text{ cm s}^{-1}$ .



Single molecule fluorescence experiments are now widely used to detect and characterize biological molecules, one by one, as they diffuse through a confocal probe volume defined by focused laser beams.<sup>1</sup> By analyzing a large number of individual molecules it is possible to characterize different subpopulations of molecules and detect rare species. These experiments are typically carried out in a static volume at sample concentrations of around  $100 \text{ pM}$ , using laser powers of a few hundred microwatts. The sample concentration is kept low to minimize the probability of two molecules simultaneously occupying the probe volume, while the irradiance is limited to avoid attenuation of signal by processes such as photobleaching and population of triplet states.<sup>2</sup> The use of nanofabricated structures reduces the probe volume further, allowing single molecule measurements to be made at concentrations up to  $10 \mu\text{M}$ .<sup>3</sup> However, the detection of rare analytes (e.g., at femtomolar concentrations) with confocal optical systems requires extended acquisition times, due to the low diffusion-limited encounter rate of dilute species with the femtoliter-sized detection volume.

Alternatively, experiments can be performed on flowing molecules.<sup>4–6</sup> This approach, analogous to flow cytometry, has many potential advantages over measurements on a static volume. The use of multifunctional devices for sample manipulations enable experiments which cannot be performed on static samples, such as the study of biomolecular interactions using microfluidic mixers,<sup>7–9</sup> or the inhibition of oxygen-mediated photobleaching by using a permeable poly(dimethyl)siloxane (PDMS) microfluidic device to mediate gas exchange.<sup>10</sup> Additionally, the heterogeneity of the paths taken by the fluorophores through the laser focus is

reduced and the flow rate can be increased to accelerate the rate of data acquisition, which is an attractive proposition for rapid detection of rare species. However, the corollary of high speed is the reduced residence time of fluorophores in the observation volume, because the linear flow velocity greatly exceeds the velocity of random diffusion.<sup>11</sup> Since the number of emitted photons is limited by the number of excitation-relaxation cycles that fluorophores can complete in this transit time, the signal-to-noise ratio would be expected to deteriorate with increasing molecular velocity. As a result, there have only been a handful of reports of single molecule detection (SMD) at flow speeds  $>1 \text{ cm s}^{-1}$ . In early examples, large dsDNA fragments ( $\geq 10 \text{ kbp}$ ) flowing at  $1\text{--}5 \text{ cm s}^{-1}$  were detected.<sup>12,13</sup> Sufficient signal for detection was generated by staining with  $\geq 2000$  fluorescent intercalators and as a consequence of the relatively long transit time of  $\sim 1 \text{ ms}$  through the  $\sim 50 \mu\text{m}$  excitation spot. In contrast, confocal optical setups currently used for single fluorophore detection generate a beam diameter of  $\sim 500 \text{ nm}$ , which a molecule traveling at  $5 \text{ cm s}^{-1}$  would traverse in  $\sim 10 \mu\text{s}$ . More recently, detection of single Alexa Fluor 488-labeled dUTP molecules at up to  $10 \text{ cm s}^{-1}$  has been achieved using a nanofabricated channel  $\sim 350 \text{ nm}$  in diameter for sample confinement. The signal is maximized because analytes only travel through the center of the focal volume, where its intensity is greatest.<sup>14</sup>

Received: August 31, 2011

Accepted: November 18, 2011

Published: December 06, 2011

Imaging-based methods, where multiple moving molecules can be counted simultaneously using a CCD camera, achieve a higher throughput than is possible using a confocal setup due to the larger volumes that can be sampled. Again, early work relied on detection of long dsDNA labeled with >100 fluorescent intercalators,<sup>15</sup> while more recent studies have demonstrated detection of single Alexa Fluor 660 fluorophores.<sup>16</sup> Modest flow speeds ( $\sim 0.01 \text{ cm s}^{-1}$ ) are necessary to maximize signal, but the parallel nature of the measurement could allow detection of up to  $\sim 10^7$  molecules  $\text{s}^{-1}$ . However, single fluorophore detection requires the use of high numerical aperture objectives that image a small field of view, thereby reducing the theoretical throughput to  $6.7 \times 10^4$  molecules  $\text{s}^{-1}$  using five simultaneously illuminated microchannels. In this paper, we present a general method that can be used to experimentally determine the optimal flow velocities for single molecule measurements, using a confocal optical setup, for both direct counting and also for characterization of dual-labeled analytes using two-color coincidence detection (TCCD) and single pair Förster resonance energy transfer (spFRET).

## EXPERIMENTAL SECTION

**Microfluidic Device.** The PDMS microfluidic device has three inlet holes and one outlet hole (Figure S1 in the Supporting Information). Buffer injected from both side inlets hydrodynamically focus the sample solution in the center of the flow channel to minimize the adsorption of molecules to the PDMS walls. The dimensions of the device were  $100 \mu\text{m}$  in width and  $25 \mu\text{m}$  in height. Syringes (Hamilton, Gastight,  $250 \mu\text{L}$ ) were connected via polyethylene tubing (Intramedic, internal diameter  $0.38 \text{ mm}$ ) to the device. Flow control was achieved with syringe infusion pumps (Harvard Apparatus 2000). The flow rates of buffer and sample were the same. The flow speeds quoted throughout refer to the mean velocities calculated from the total flow rate and the volumetric capacity of microfluidic device.

**Bulk Fluorescence Experiments.** The brightness of duplex 1 (10 nM in TEN buffer, containing 0.01% tween-20 to prevent surface adhesion) at each detection wavelength was measured using laser powers of 0.3 or 1.3 mW at 488 and 640 nm. The flowing samples were exposed to each wavelength successively to minimize crosstalk between the detection channels. Single laser excitation at 488 nm was used at 0.3 and 1.3 mW for FRET measurements on duplex 2 in otherwise identical conditions. In both experiments, data were collected in  $100 \mu\text{s}$  time-bins using different flow speeds. The APD correction factor curve provided by the manufacturer (Perkin-Elmer, Waltham, MA) was used to correct the large signal brightness (photons/s) measured from both colors in these experiments.

**Single Molecule Measurements in Flow.** Single molecule dual-excitation coincidence experiments in flow were performed using the single molecule fluorescence microscope described in the Supporting Information. The two side channels were used for TEN buffer, and duplex 1 (50, 500, 5 000, 50 000, or 500 000 fM in TEN buffer, containing 0.01% tween-20 to prevent surface adhesion) was flowed through the middle channel. For FRET experiments, duplex 2 (50, 500, 5 000, or 50 000 fM), duplex 3 (5 000 fM), or duplex 4 (5 000 fM) was flowed through the central channel under identical conditions except that only the 488 nm laser was used for excitation, generating a FRET signal in the red channel. All data were collected for 4 min after waiting 3 min following the initiation of sample infusion and the averages

from three replicate measurements are reported. The laser powers, time bins, and thresholds used for all experiments are given in the Supporting Information (Tables S2 and S3), as are details of methods used for data analysis.

## RESULTS AND DISCUSSION

### Bulk Fluorescence Measurements of Flowing Molecules.

It has long been known that photoisomerization/photodestruction of chromophores can be inhibited by using rapid flow to limit the duration of their exposure to the illuminating beam. This approach enabled the Raman spectra of rhodopsin and isorhodopsin to be obtained<sup>17</sup> and has been used to measure flow velocities in microfluidic devices.<sup>18</sup> Related phenomena in single molecule fluorescence spectroscopy are the higher quantum efficiencies seen at low laser powers<sup>19</sup> and when quickly scanning the laser beam through a static solution.<sup>20</sup> These increases in brightness result from a reduction in the number of excitation cycles completed by each fluorophore, leading to the suppression of photophysical processes that compete with fluorescence, such as photobleaching or blinking. It is therefore expected that flowing molecules should emit photons for a greater fraction of their occupation time than diffusing species.

We analyzed the effect of flow speed on the signal obtained from two organic dyes commonly used for single molecule experiments, Alexa Fluor 488 and Alexa Fluor 647, at a concentration of 10 nM. Under these conditions, the same number of molecules are present in the laser focus on average ( $\sim 3$  molecules assuming a detection volume of  $0.5 \text{ fL}$ ), but their residence time is reduced with increasing flow speed. Working in this bulk regime avoids any issues arising from dependence of the mean brightness on thresholds or comparing data taken with different bin times. We studied the effect of flow velocities from 0 to  $9 \text{ cm s}^{-1}$  on the brightness of dual-labeled DNA duplex 1 at laser powers of 0.3 and 1.3 mW. The results (Figure 1B) show a sharp increase in the brightness of both fluorophores between 0 and  $0.5 \text{ cm s}^{-1}$  and a gradual increase at higher speeds. These two regimes could be due to transitions to different nonfluorescent states whose populations reach equilibrium at different rates, depending on the quantum yield of blinking/bleaching. When the brightness is plotted against the reciprocal of the flow speed (proportional to the residence time, Figure 1C), a biphasic decay is apparent for both fluorophores. The faster phase equilibrates at velocities  $\leq 100 \mu\text{s}/\mu\text{m}$  (corresponding to residence times of  $\leq 50 \mu\text{s}$  for molecules traversing a  $500 \text{ nm}$  probe volume) and the slower one, which becomes more significant at higher excitation irradiance, operates over  $100\text{--}1000 \mu\text{s}/\mu\text{m}$ . We tentatively attribute the faster process to intersystem crossing, leading to population of the lowest excited triplet state and the slower one to photobleaching. Given its higher apparent yield at the higher power density, the slower process may involve absorption of a second photon by an excited fluorophore, as in two-step photolysis.<sup>21</sup> Other possible attenuating processes include photoisomerization of the cyanine Alexa Fluor 647 dye<sup>22</sup> or a photochemically induced red-shift in the emission of Alexa Fluor 488.<sup>23</sup> Further experiments will be required to determine the precise origin of the effects observed in our data; such a study is beyond the scope of this paper.

**Single Molecule Detection in Flow.** Notably, the observed enhancement in bulk fluorescence brightness in flow was much greater at the higher laser power of 1.3 mW ( $\sim 10$ -fold) than at 0.3 mW ( $\sim 2$ -fold). We therefore reasoned that the optimal

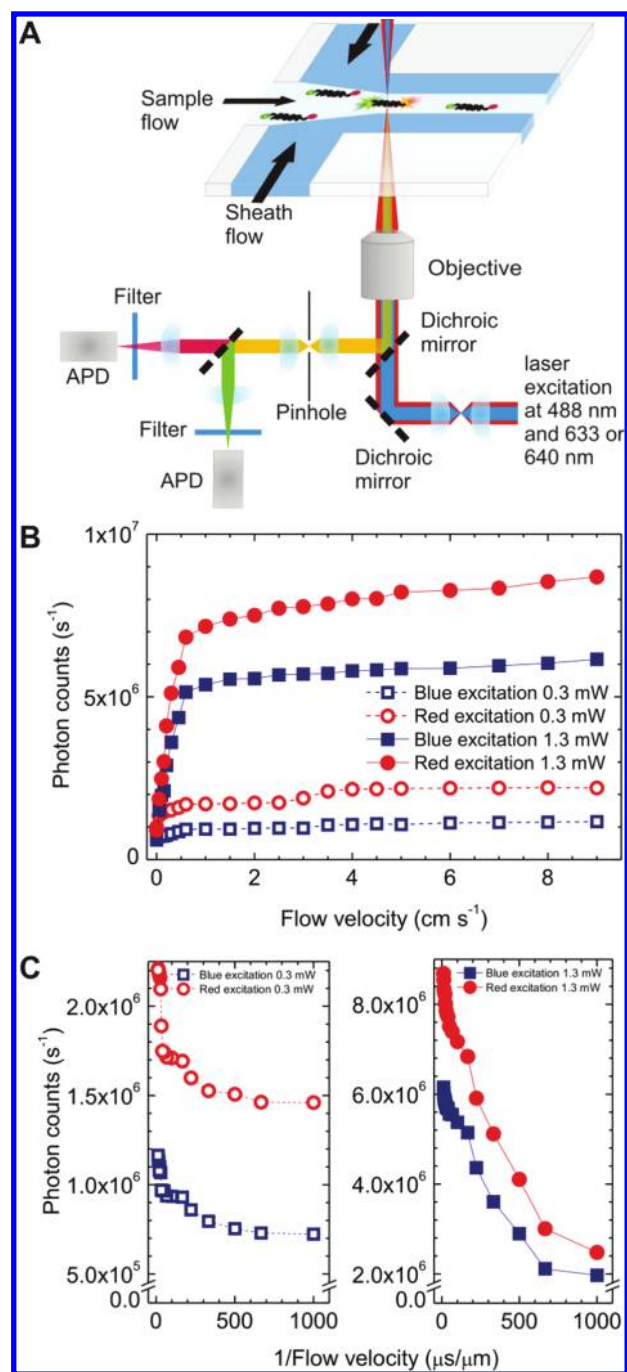


**Figure 1.** (A) Schematic of the experimental setup, consisting of an inverted confocal fluorescence microscope interfaced with a flow cell. Single laser excitation was used for Förster resonance energy transfer (FRET) studies, while two color coincidence detection (TCCD) was achieved using dual laser excitation, as described previously.<sup>24</sup> The microfluidic device was fabricated using standard soft lithographic methods.<sup>25</sup> (B) Variation of the average dye brightness with flow velocity at a sample concentration of 10 nM, using a 100  $\mu$ s time bin. A neutral density filter (OD = 1) was used to attenuate the signal reaching the APDs. Using static samples (0 cm s<sup>-1</sup>), the mean brightness of blue-excited fluorescence was  $6 \times 10^5$  and  $7 \times 10^5$  counts s<sup>-1</sup>, at powers of 0.3 and 1.3 mW, while the mean brightness of red-excited fluorescence was  $1 \times 10^6$  and  $9 \times 10^5$  counts s<sup>-1</sup> at 0.3 and 1.3 mW. (C) Mean brightness of blue- and red-excited fluorescence at both excitation powers plotted against the reciprocal of the flow velocity.

irradiance might vary with flow velocity. Furthermore, in two-color excitation or FRET experiments, photobleaching due to absorption of a blue excitation photon by the excited red fluorophore state adds a photophysical pathway not present in the single-color excitation we used for bulk measurements of fluorescence intensities.<sup>26</sup> As a result, SMD at each flow velocity was initially carried out at a variety of intensities (data not shown) and that which resulted in the largest brightness of fluorescence bursts in each channel used in further experiments (Table S2 in the Supporting Information). Representative data obtained from two-color excitation of a 5 pM sample of duplex 1, collected using the optimal laser powers, are shown for flow velocities of 0 (i.e., molecules undergoing diffusion), 1, and 10 cm s<sup>-1</sup> (Figure 2A). Contour plots of all bursts obtained are available as Supporting Information (Figures S3 and S4). The trade-offs inherent in the method are clearly apparent; with increasing velocity, the volume of data collected increases substantially, while the brightness of individual bursts decrease. The key question we sought to answer in this work is: What is the optimal flow speed for single molecule measurements? To address this we used three parameters obtained from model samples to evaluate the quality of data obtained at different flow velocities: the association quotient ( $Q$ ), the rate at which coincident events are observed and the appearance of intensity ratio histograms.

In order to process the data to obtain these parameters, it was first necessary to select time bins and thresholds suitable for identifying a burst of fluorescence due to single molecules while rejecting noise due to scattering or autofluorescent impurities. Time bins were selected according to the expected residence time of molecules traveling at each velocity in the confocal volume, which has a beam waist of approximately 500 nm; their validity was confirmed by the vast majority of events (>90% in all experiments on flowing molecules) being restricted to a single time bin (Tables S2 and S3 in the Supporting Information). Because of the variation in residence times, brightness, and excitation irradiance, we found a nonlinear dependence of burst intensity on flow speed that complicates the selection of thresholds which allow comparison of data collected at different velocities. We solved this problem by the use of an automated method that selects the thresholds for each data set that maximize the association quotient ( $Q$ ), the ratio of the rate of significant coincident events (i.e., above that expected by chance) to the total event rate. We have previously shown that this approach enables quantification of dual-labeled DNA in a static volume using different laser powers.<sup>19</sup> We therefore used this method to set the thresholds (Table S2 in the Supporting Information) at each flow speed and then compared the resulting data.

The association quotient ( $Q$ ) calculated for TCCD or FRET data indicates the fraction of events that exhibit bursts of fluorescence above the threshold simultaneously in both detection channels. For both model samples we measured,  $Q$  was found to be  $\sim 0.2$  in a static volume, as expected due to the mismatch in excitation and detection volumes for each fluorophore.<sup>27,28</sup> In TCCD (Figure 2B),  $Q$  was then found to increase to 0.23 at 0.5 cm s<sup>-1</sup> and decrease steadily at higher speeds, falling by  $\sim 50\%$  at 4 cm s<sup>-1</sup>. This slight initial increase can be rationalized as the result of a reduction in photophysical processes competing with fluorescence, which increases the probability of both dyes being in an emissive state during the measurement. The decrease in  $Q$  observed at higher velocities is most likely caused by the reduced event brightness due to the shorter residence time of the molecules in the confocal volume. This increases the chance of

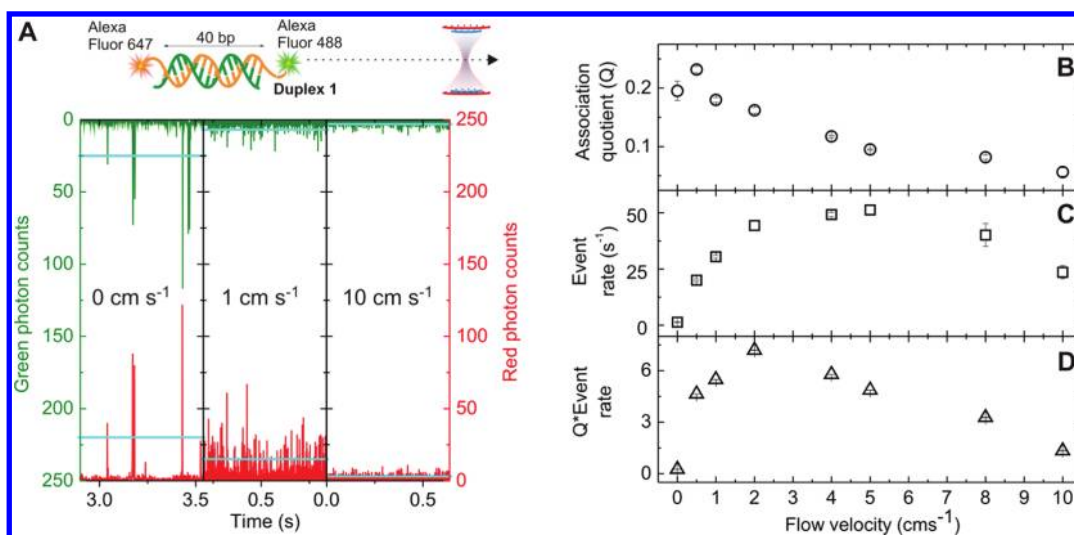


**Figure 2.** TCCD in microfluidic flow: (A) Representative two color single molecule data from dual-labeled duplex 1 (5 pM) taken at flow velocities of 0, 1, and 10  $\text{cm s}^{-1}$  (using time bins of 1 ms, 100  $\mu\text{s}$ , and 10  $\mu\text{s}$ , respectively). A total of 640 ms of data are shown in each panel. The thresholds on each channel that maximize the association quotient<sup>19</sup> are indicated by the horizontal lines. Plots of association quotient (B), coincident event rate (C), and the product of association quotient and event rate (D) against flow velocity obtained from a 5 pM solution of duplex 1.

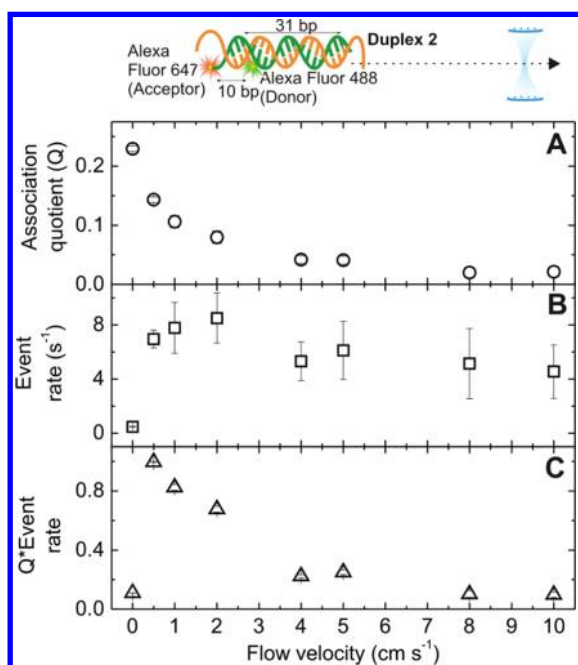


**Figure 3.** spFRET in microfluidic flow. Plots of association quotient (A), coincident event rate (B), and the product of association quotient and event rate (C) against flow velocity obtained from a 5 pM solution of duplex 2.

the signal from one of the fluorophores being below the threshold. In spFRET measurements (Figure 3A),  $Q$  decreases exponentially with flow velocity, dropping by  $\sim 50\%$  at 1  $\text{cm s}^{-1}$ . The fact that the detection efficiency in spFRET falls more sharply than in TCCD can be understood by considering that only the donor directly absorbs excitation photons during the detection process, which then gives rise to emission by either the donor or the acceptor. In contrast, the two chromophores may absorb excitation photons independently in TCCD. The likelihood of the detected brightness being below the event threshold in either

detection channel therefore increases more quickly with flow speed in spFRET experiments.

Our main motivation for making measurements on flowing molecules was to increase the rate at which single molecule data could be acquired. As can be seen from Figures 2C and 3B, the coincident event rate can be increased significantly to a maximum (38-fold in TCCD, at 5  $\text{cm s}^{-1}$  and 18-fold in FRET, at 2  $\text{cm s}^{-1}$ ), before declining at higher velocities. Since the maximum event rates are observed at higher speeds than the maximum association quotient, the increased encounter rate of flowing molecules with the probe volume can initially compensate for the dimmer bursts obtained due to their reduced residence time. When the velocity is increased further, the detection efficiency becomes so low that the rate of significant events drops despite the fact that analytes encounter the confocal volume more frequently. The trade-off between these two factors is illustrated in Figures 2D and 3C, where the product of coincident event rate and  $Q$  is plotted against flow velocity, reaching a maximum at 2  $\text{cm s}^{-1}$  for TCCD and 0.5  $\text{cm s}^{-1}$  for FRET detection.

Two-color histograms are typically plotted from single molecule data in order to obtain structural information about the system under study; this may consist of the stoichiometry of complexes determined by TCCD<sup>29</sup> or the elucidation of molecular conformations by spFRET.<sup>30,31</sup> In either method, the presence of structurally distinct subpopulations is indicated by multiple Gaussian distributions in these histograms. Since microfluidic flow enables acceleration of the molecule-sampling rate, its use should allow this type of information to be accessed much more quickly, provided that the data are not compromised as a result of the decrease in burst brightness. Selected TCCD and FRET two-color histograms are shown in Figure 4A (complete sets are available in the Supporting Information, Figures S7–S9). The log-normal TCCD histograms obtained from dual-labeled duplex 1 undergoing diffusion or flowing at 1  $\text{cm s}^{-1}$  are both fit by a Gaussian distribution, with a slightly better fit observed for the latter due to the increase in the number of data points acquired over the fixed measurement period. This increases the measurement precision by reducing the “molecular shot-noise”,

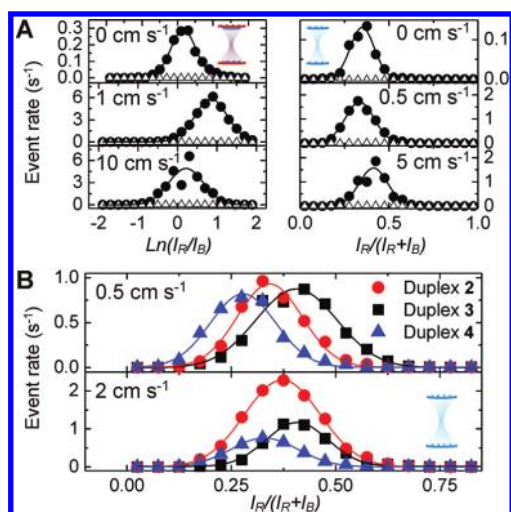


**Figure 4.** (A) Averaged log-normal TCCD (left panels, recorded at 0, 1, and 10 cm s<sup>-1</sup>) and FRET proximity ratio histograms (right panels, recorded at 0, 0.5, and 5 cm s<sup>-1</sup>). Data were recorded from a 5 pM solution of duplex 1 (TCCD) or 2 (FRET). For comparison, data collected from buffer over the same acquisition period using the same thresholds are also shown ( $\Delta$ ). (B) Resolution of different donor–acceptor distances by spFRET at two flow velocities. Averaged proximity ratio histograms were recorded at 0.5 cm s<sup>-1</sup> (top panel) and 2 cm s<sup>-1</sup> (lower panel) from a 5 pM solution of duplex 2 (10 bp interfluorophore separation), 3 (8 bp separation), and 4 (15 bp separation).

the uncertainty resulting from stochastic variations in the number of molecules sampled.<sup>32</sup> When the flow velocity is increased further to 10 cm s<sup>-1</sup>, a similar sampling rate is achieved but the distribution is poorly fit by a Gaussian function. This loss of precision therefore does not result from molecular shot-noise but an increase in photon shot-noise due to the reduced counts obtained from very fast-flowing molecules (mean total event brightness = 10.7 counts/bin at 10 cm s<sup>-1</sup>, compared with 39.6 counts/bin when flowing at 1 cm s<sup>-1</sup>). This finding is in good agreement with the work of Gopich and Szabo, which has shown that FRET efficiency histograms exhibit broadening and a noisy appearance when the total number of collected photons is fewer than 20, due to the limited number of combinations of integer values in each channel.<sup>33</sup>

Similar trends are observed for the spFRET proximity ratio histograms, though the quality of data deteriorate at slower flow speeds than for dual-excitation. However, at flow speeds  $\leq 2$  cm s<sup>-1</sup>, similar peak positions and distribution widths are observed, indicating that high illumination intensity does not affect the measurement, reflecting the longer fluorescence lifetime of the donor, Alexa Fluor 488 (4.1 ns), than the acceptor, Alexa Fluor 647 (1.0 ns). The histograms recorded at  $\geq 4$  cm s<sup>-1</sup> are slightly narrowed and shifted toward 0.5. A reduction in FRET histogram width has previously been observed in “molecular cytometry”,<sup>34</sup> which might be explained by the fact that histograms are broadened by photophysical processes other than emission of fluorescence.<sup>35</sup> However, the narrowing and red-shift observed in our experiments at  $\geq 4$  cm s<sup>-1</sup> is most likely an artifact resulting from thresholding a set of low photon counts (e.g., mean total event brightness = 19.0 photon counts/bin at 5 cm s<sup>-1</sup>), leading to a small distribution of observed values above the threshold (e.g., 5 and 4 photon counts/bin at 5 cm s<sup>-1</sup> for donor and acceptor events, respectively). This explanation is supported by the fact that in

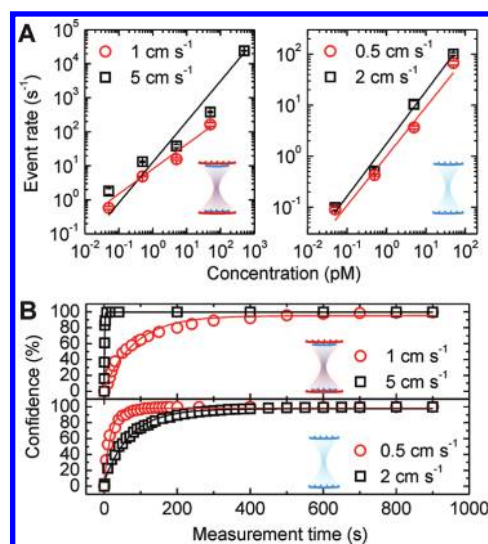


**Figure 5.** Detection of dual-labeled DNA by single molecule counting in flow. (A) Plots of the dependence of the rate of significant coincidence bursts on sample concentration measured from duplex 1 by TCCD (left panel, recorded at 1 and 5 cm s<sup>-1</sup>) and from duplex 2 by FRET (right panel, recorded at 0.5 and 2 cm s<sup>-1</sup>). The coincident event rates detected from buffer at each flow velocity are given in Table S4 in the Supporting Information. (B) Statistical confidence of detection of dual-labeled DNA at 50 fM, based on the Poisson-distributed number of coincident events detected from the sample and buffer, calculated according to eq 6 (Supporting Information). The variation of statistical confidence with measurement time is shown for duplex 1 (top panel, detected by TCCD at 1 and 5 cm s<sup>-1</sup>) and duplex 2 (lower panel, detected by FRET at 0.5 and 2 cm s<sup>-1</sup>).

bulk measurement, where no thresholds are used and high photon counts are recorded, the proximity ratio does not vary significantly with flow velocity (Figure S2 in the Supporting Information).

We further investigated the quality of structural information obtained by SMD in flow by comparing the resolution of different donor–acceptor separations in DNA duplexes. Proximity ratio histograms were recorded at two different flow speeds from duplexes in which the donor (Alexa Fluor 488) and the acceptor (Alexa Fluor 647) were separated by 8, 10, or 15 bp (Figure 4B). We chose flow velocities of 0.5 cm s<sup>-1</sup>, where the highest association quotient in flow was observed, and 2 cm s<sup>-1</sup>, which gave the maximum event rate. The positions of the peaks in the resultant Gaussian distributions are well separated at 0.5 cm s<sup>-1</sup> but converge at 2 cm s<sup>-1</sup>, making it difficult to distinguish the different species. This result underlines the message that the information content of single molecule data is degraded at very high flow velocities by photon shot-noise, impairing the ability to recover structural detail. As a result, care should be taken when using fast flow to analyze species with high or low FRET efficiencies, as low photon counts are obtained in one of the detection channels.

**Detection of Flowing Analytes by Burst Counting.** Although structural characterization is the goal of many SMD experiments, in applications such as molecular diagnostics it is the quantification of biomolecular targets such as nucleic acids or proteins by molecule counting that is of primary importance.<sup>36–38</sup> We counted coincident bursts from duplexes 1 (TCCD) and 2 (FRET) at concentrations between 50 fM and 500 pM at two flow velocities: one that gave high quality histograms (1 cm s<sup>-1</sup> for TCCD and 0.5 cm s<sup>-1</sup> for FRET) and the one which gave the maximum event rate (5 cm s<sup>-1</sup> for TCCD and 2 cm s<sup>-1</sup> for FRET). A linear

dependence of coincident event rate on concentration was observed in all experiments, spanning a dynamic range of 3 orders of magnitude (50 fM–50 pM, Figure 5A). Using TCCD at 5 cm s<sup>-1</sup> enabled SMD at the highest concentration of 500 pM, but in all other cases it was not possible to resolve single molecule bursts at this concentration. It is likely that the dimmer bursts observed at the higher flow velocity enable maintenance of a single molecule detection regime at higher concentrations; since fluorophores encountering the less intense peripheries of the laser focus do not generate detectable signals during their short residence time, the effective detection volume becomes smaller.

The precision in the measured concentration of analyte is of critical importance in molecule counting applications and depends not only on the number of events observed due to the sample but also the number of events in the absence of analyte due to background noise. We calculated the measurement times required to detect the lowest concentration studied (50 fM) with high confidence using a method based on Poisson statistics that we and others have previously used to evaluate molecule counting studies.<sup>27,39</sup> The increase in statistical confidence with measurement time is shown in Figure 5B for TCCD (at 1 and 5 cm s<sup>-1</sup>) and FRET detection (at 0.5 and 2 cm s<sup>-1</sup>), while the acquisition times required to reach a 99.5% confidence interval are reported in Table S4 in the Supporting Information. Using TCCD, this period dropped from 900 to 8 s when the flow velocity was increased from 1 to 5 cm s<sup>-1</sup>, due to the increased event rate. When single-color excitation is used, detection at 0.5 cm s<sup>-1</sup> can be accomplished more quickly (170 s) than using dual-color excitation at 1 cm s<sup>-1</sup>, largely due to the lower background event rate obtained. However, when the flow velocity is increased to 2 cm s<sup>-1</sup>, the detection time (650 s) lengthened significantly compared to two-color excitation at 10 cm s<sup>-1</sup>, despite the background rate being higher in TCCD. This observation is the result of the reduced detection efficiency possible with spFRET in fast flow.

## CONCLUSIONS

In this study, we have addressed the fundamental question of how fast it is possible to flow analytes and still extract useful data from single molecule fluorescence experiments. When the molecules are driven through the probe volume using a microfluidic device, the rate at which coincident events are detected increases substantially, reaching a maximal enhancement of 38-fold with two-color excitation/detection at 5 cm s<sup>-1</sup> and 18-fold for FRET detection at 2 cm s<sup>-1</sup>. These flow speeds represent the fastest rate at which single molecules can be counted using confocal detection. At higher velocities, the event rate falls because the reduced residence time of analytes within the confocal volume leads to fewer emitted photons. The quality of two-color and proximity ratio histograms improve at moderate flow velocities due to the increase in volume of data collected compared with diffusion but deteriorate at flow velocities beyond 2 cm s<sup>-1</sup> (using two-color excitation/detection) or 1 cm s<sup>-1</sup> (using spFRET detection). These velocities represent the fastest rate at which single molecules can be characterized using confocal detection.

On the other hand, TCCD in fast flow can enable rapid quantification of dilute analytes, even when structural information can no longer be accessed. The detection of 50 fM DNA with 99.5% confidence in 8 s by TCCD using a flow velocity of 5 cm s<sup>-1</sup> is a dramatic improvement on our previous work, where a measurement time of 60 min was required to detect 100 fM

dual-labeled DNA undergoing diffusion with 99% confidence.<sup>27</sup> It is also significantly faster than the ~70 s required for detection of 700 fM unlabeled DNA hybridized to Molecular Beacons with 99% accuracy reported by Wang et al., using a much more complicated microfluidic device that incorporates microelectrodes to enable molecular focusing by dielectrophoresis.<sup>39</sup> Although the detection efficiency achieved using that device is greater than we obtain here, the faster flow velocity we use increases the event rate (13.2 s<sup>-1</sup> with 500 fM dual-labeled DNA, compared with 2.15 s<sup>-1</sup> for 700 fM hybridized unlabeled DNA, using Wang's device) and the coincidence criterion we apply produces a much lower background event rate (0.067 s<sup>-1</sup>) than that due to unhybridized Molecular Beacons (1.35 s<sup>-1</sup>). It is also likely that some of the difference between these two methods results from the increased complexity of the sample detected by Wang et al., which is closer to a real diagnostic assay than the model samples we have studied here. The sample event rate they observe could be reduced by inefficiency in Molecular Beacon hybridization and the background event rate raised by the presence of free dye or incorrectly folded Molecular Beacons. Nevertheless, it should be possible to complete assays such as these much more rapidly using the optimized conditions we report here. It would be interesting to use our coincidence-based detection of unlabeled DNA in fast flow by sandwich hybridization with two dye-labeled ssDNA probes<sup>36,40</sup> or Molecular Beacons.<sup>41</sup>

The speeds we have defined in this work are likely to be close to the absolute limits for single molecule detection, but there may be some incremental improvements possible. For example, the use of nanofluidic channels to force analytes through the most intense central part of the probe volume, as previously described by Foquet et al.,<sup>14</sup> should increase the detection efficiency at high flow velocities. Alternatively, the use of multiply labeled species or brighter fluorophores would allow higher velocities to be used. We have previously characterized a variety of samples with multiple fluorophores, using TCCD to assay telomere repeat sequences bearing up to seven cyanine dyes,<sup>42</sup> as well as single virions labeled with several hundred fluorophores,<sup>43</sup> and FRET to characterize amyloidogenic protein oligomers containing around 38 labels.<sup>44</sup> Furthermore, Stavis et al. have shown that bursts recorded from flowing quantum dots are about three times as intense as those from the organic Alexa Fluor 488 dye used in our study.<sup>45</sup> However, given the widespread use of these and similar fluorophores and the fact that the improvements we disclose can be obtained using a relatively simple microfluidic device, we expect that our simple approach could be exploited quickly and easily by many researchers currently making single molecule fluorescence measurements on diffusing molecules.

This study shows that high throughput counting of single molecules (~2.4 × 10<sup>4</sup> molecules s<sup>-1</sup> in one channel) is possible using confocal optics. The wide microfluidic channels (100 μm) we have used simplify the fabrication process but lead to low detection efficiency due to the size mismatch with the illuminated area (with a diameter < 1 μm). For experiments where the sample volume is limited (e.g., in some diagnostic applications), the detection efficiency could be improved by the use of sample confinement<sup>14,39</sup> or sheet-like illumination schemes<sup>38,46</sup> while maintaining the same throughput.

The high signal-to-noise ratio obtained using confocal measurements can yield parameters such as FRET efficiency or stoichiometry as well as the quantification offered by molecule counting. Though slightly slower flow speeds must be used to access such information, one could envisage detecting low populations of

molecules of interest, such as protein oligomers during aggregation, using high flow velocity to achieve maximal throughput, and adjusting the flow rate to enable structural characterization.

## ■ ASSOCIATED CONTENT

**S Supporting Information.** Protocol for fabrication of microfluidic devices, description of single molecule fluorescence microscope, sequences of synthetic oligonucleotides, details of data analysis methods, additional data, Tables S1–S4, and Figures S1–S9. This material is available free of charge via the Internet at <http://pubs.acs.org>.

## ■ AUTHOR INFORMATION

### Corresponding Author

\*E-mail: [dk10012@cam.ac.uk](mailto:dk10012@cam.ac.uk).

## ■ ACKNOWLEDGMENT

M.H.H., H.L., and J.-u.S. contributed equally to this work, which was funded by the EU (TheraEDGE Network Contract FP7-216027), BBSRC, and EPSRC. J.-u.S. thanks the EU for a Marie-Curie fellowship. M.H.H. thanks the Royal Society of Chemistry (Analytical Chemistry Trust Fund) for his student-ship. The authors thank Angel Orte (University of Granada) for his critical reading of the manuscript.

## ■ REFERENCES

- Cornish, P. V.; Ha, T. *ACS Chem. Biol.* **2007**, *2*, 53–61.
- Dittrich, P. S.; Schwille, P. *Appl. Phys. B: Lasers Opt.* **2001**, *73*, 829–837.
- Levene, M. J.; Korfach, J.; Turner, S. W.; Foquet, M.; Craighead, H. G.; Webb, W. W. *Science* **2003**, *299*, 682–686.
- Nguyen, D. C.; Keller, R. A.; Jett, J. H.; Martin, J. C. *Anal. Chem.* **1987**, *59*, 2158–2161.
- Dovichi, N. J.; Martin, J. C.; Jett, J. H.; Trkula, M.; Keller, R. A. *Anal. Chem.* **1984**, *56*, 348–354.
- Barnes, M. D.; Lermer, N.; Kung, C. K.; Whitten, W. B.; Ramsey, J. M.; Hill, S. C. *Opt. Lett.* **1997**, *22*, 1265–1267.
- Lipman, E. A.; Schuler, B.; Bakajin, O.; Eaton, W. A. *Science* **2003**, *301*, 1233–1235.
- Gambin, Y.; VanDelinder, V.; Ferreone, A. C. M.; Lemke, E. A.; Groisman, A.; Deniz, A. A. *Nat. Methods* **2011**, *8*, 239–241.
- Kim, S.; Streets, A. M.; Lin, R. R.; Quake, S. R.; Weiss, S.; Majumdar, D. S. *Nat. Methods* **2011**, *8*, 242–245.
- Lemke, E. A.; Gambin, Y.; Vandelinder, V.; Brustad, E. M.; Liu, H. W.; Schultz, P. G.; Groisman, A.; Deniz, A. A. *J. Am. Chem. Soc.* **2009**, *131*, 13610–13612.
- Chao, S. Y.; Ho, Y. P.; Bailey, V. J.; Wang, T. H. *J. Fluoresc.* **2007**, *17*, 767–774.
- Goodwin, P. M.; Johnson, M. E.; Martin, J. C.; Ambrose, W. P.; Marrone, B. L.; Jett, J. H.; Keller, R. A. *Nucleic Acids Res.* **1993**, *21*, 803–806.
- Larson, E. J.; Hakovirta, J. R.; Cai, H.; Jett, J. H.; Burde, S.; Keller, R. A.; Marrone, B. L. *Cytometry* **2000**, *41*, 203–208.
- Foquet, M.; Korfach, J.; Zipfel, W. R.; Webb, W. W.; Craighead, H. G. *Anal. Chem.* **2004**, *76*, 1618–1626.
- Anazawa, T.; Matsunaga, H.; Yeung, E. S. *Anal. Chem.* **2002**, *74*, 5033–5038.
- Okagbare, P. I.; Soper, S. A. *Analyst* **2009**, *134*, 97–106.
- Mathies, R.; Oseroff, A. R.; Stryer, L. *Proc. Natl. Acad. Sci. U.S.A.* **1976**, *73*, 1–5.
- Wang, G. R. *Lab Chip* **2005**, *5*, 450–456.
- Clarke, R. W.; Orte, A.; Klenerman, D. *Anal. Chem.* **2007**, *79*, 2771–2777.
- Vukojevic, V.; Heidkamp, M.; Ming, Y.; Johansson, B.; Terenius, L.; Rigler, R. *Proc. Natl. Acad. Sci. U.S.A.* **2008**, *105*, 18176–18181.
- Egging, C.; Widengren, J.; Rigler, R.; Seidel, C. A. M. *Anal. Chem.* **1998**, *70*, 2651–2659.
- White, S. S.; Li, H.; Marsh, R. J.; Piper, J. D.; Leonczek, N. D.; Nicolaou, N.; Bain, A. J.; Ying, L.; Klenerman, D. *J. Am. Chem. Soc.* **2006**, *128*, 11423–11432.
- Chung, H. S.; Louis, J. M.; Eaton, W. A. *Proc. Natl. Acad. Sci. U.S.A.* **2009**, *106*, 11837–11844.
- Orte, A.; Clarke, R.; Balasubramanian, S.; Klenerman, D. *Anal. Chem.* **2006**, *78*, 7707–7715.
- Sia, S. K.; Whitesides, G. M. *Electrophoresis* **2003**, *24*, 3563–3576.
- Kong, X.; Nir, E.; Hamadani, K.; Weiss, S. *J. Am. Chem. Soc.* **2007**, *129*, 4643–4654.
- Li, H.; Ying, L. M.; Green, J. J.; Balasubramanian, S.; Klenerman, D. *Anal. Chem.* **2003**, *75*, 1664–1670.
- Orte, A.; Clarke, R. W.; Klenerman, D. *Anal. Chem.* **2008**, *80*, 8389–8397.
- Alves, D.; Li, H. T.; Codrington, R.; Orte, A.; Ren, X. J.; Klenerman, D.; Balasubramanian, S. *Nat. Chem. Biol.* **2008**, *4*, 287–289.
- Schuler, B.; Lipman, E. A.; Eaton, W. A. *Nature* **2002**, *419*, 743–747.
- Deniz, A. A.; Laurence, T. A.; Beligere, G. S.; Dahan, M.; Martin, A. B.; Chemla, D. S.; Dawson, P. E.; Schultz, P. G.; Weiss, S. *Proc. Natl. Acad. Sci. U.S.A.* **2000**, *97*, 5179–5184.
- Chen, D.; Dovichi, N. J. *Anal. Chem.* **1996**, *68*, 690–696.
- Gopich, I.; Szabo, A. *J. Chem. Phys.* **2005**, *122*, 014707.
- Werner, J. H.; McCarney, E. R.; Keller, R. A.; Plaxco, K. W.; Goodwin, P. M. *Anal. Chem.* **2007**, *79*, 3509–3513.
- Kalinin, S.; Sisamak, E.; Magennis, S. W.; Felekyan, S.; Seidel, C. A. M. *J. Phys. Chem. B* **2010**, *114*, 6197–6206.
- Castro, A.; Williams, J. G. K. *Anal. Chem.* **1997**, *69*, 3915–3920.
- Cipriany, B. R.; Zhao, R. Q.; Murphy, P. J.; Levy, S. L.; Tan, C. P.; Craighead, H. G.; Soloway, P. D. *Anal. Chem.* **2010**, *82*, 2480–2487.
- Huang, B.; Wu, H. K.; Bhaya, D.; Grossman, A.; Granier, S.; Kobilka, B. K.; Zare, R. N. *Science* **2007**, *315*, 81–84.
- Wang, T.-H.; Peng, Y.; Zhang, C.; Wong, P. K.; Ho, C.-M. *J. Am. Chem. Soc.* **2005**, *127*, 5354–5359.
- Agrawal, A.; Zhang, C.; Byassee, T.; Tripp, R. A.; Nie, S. *Anal. Chem.* **2006**, *78*, 1061–1070.
- Földes-Papp, Z.; Kinjo, M.; Tamura, M.; Birch-Hirschfeld, E.; Demel, U.; Titz, G. P. *Exp. Mol. Pathol.* **2005**, *78*, 177–189.
- Ren, X.; Li, H.; Clarke, R. W.; Alves, D. A.; Ying, L.; Klenerman, D.; Balasubramanian, S. *J. Am. Chem. Soc.* **2006**, *128*, 4992–5000.
- Clarke, R. W.; Monnier, N.; Li, H.; Zhou, D.; Browne, H.; Klenerman, D. *Biophys. J.* **2007**, *93*, 1329–1337.
- Orte, A.; Birkett, N. R.; Clarke, R. W.; Devlin, G. L.; Dobson, C. M.; Klenerman, D. *Proc. Natl. Acad. Sci. U.S.A.* **2008**, *105*, 14424–14429.
- Stavis, S. M.; Edell, J. B.; Samiee, K. T.; Craighead, H. G. *Lab Chip* **2005**, *5*, 337–343.
- Liu, K. J.; Wang, T.-H. *Biophys. J.* **2008**, *95*, 2964–2975.